JCI insight

Molecular mechanism responsible for sex differences in electrical activity of mouse pancreatic β cells

Noelia Jacobo-Piqueras, … , Stefanie M. Geisler, Petronel Tuluc

JCI Insight. 2024;9(6):e171609. https://doi.org/10.1172/jci.insight.171609.

Research Article | Cell biology | Endocrinology

Graphical abstract

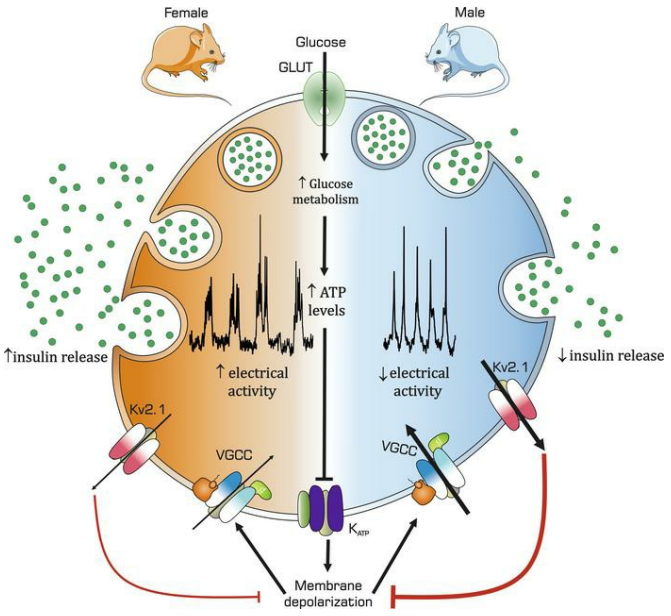

Find the latest version:

https://jci.me/171609/pdf

JCI insight

RESEARCH ARTICLE

Molecular mechanism responsible for sex differences in electrical activity of mouse pancreatic β cells

Noelia Jacobo-Piqueras, Tamara Theiner, Stefanie M. Geisler, and Petronel Tuluc

Department of Pharmacology and Toxicology, Institute for Pharmacy, University of Innsbruck, Innsbruck, Austria.

In humans, type 2 diabetes mellitus shows a higher prevalence in men compared with women, a phenotype that has been attributed to a lower peripheral insulin sensitivity in men. Whether sex-specific differences in pancreatic β cell function also contribute is largely unknown. Here, we characterized the electrophysiological properties of β cells in intact male and female mouse islets. Elevation of glucose concentration above 5 mM triggered an electrical activity with a similar glucose dependence in β cells of both sexes. However, female β cells had a more depolarized membrane potential and increased firing frequency compared with males. The higher membrane depolarization in female β cells was caused by approximately 50% smaller $K_V2.1$ K^+ currents compared with males but otherwise unchanged K_{ATP}, large-conductance and small-conductance Ca^{2+}-activated K^+ channels, and background TASK1/TALK1 K^+ current densities. In female β cells, the higher depolarization caused a membrane potential–dependent inactivation of the voltage-gated Ca^{2+} channels (Ca_V), resulting in reduced Ca^{2+} entry. Nevertheless, this reduced Ca^{2+} influx was offset by a higher action potential firing frequency. Because exocytosis of insulin granules does not show a sex-specific difference, we conclude that the higher electrical activity promotes insulin release in females, improving glucose tolerance.

Introduction

Type 2 diabetes mellitus (T2DM) is a heterogeneous disease characterized by chronic high blood glucose levels caused by impaired insulin release or its effects. In humans, T2DM has a higher incidence in males compared with females (1–4), a phenotype recapitulated by many rodent models (5–9). While different insulin sensitivity can account for this phenomenon, we hypothesize that hitherto uncharacterized sex differences in pancreatic β cell insulin release are also a critical contributor. β Cells of mice and men express a plethora of ion channels that control the glucose-induced electrical activity and insulin vesicle exocytosis (10–14). The glucose-dependent depolarization of the membrane potential (MP) is inversely controlled by the activity of ATP-sensitive K^+ channels (K_{ATP}) (15, 16). β Cell glucose uptake and metabolism increase the cytosolic ATP/ADP ratio that almost completely blocks the K_{ATP} channels in extracellular glucose levels higher than 10 mM (17). However, even when the K_{ATP} channels are completely blocked, the β cell MP remains below –40 mV, owing to the activity of background TASK-1 (18) and TALK-1 (19) 2-pore K^+ channels (K_2P). The glucose-dependent MP depolarization activates the high-voltage-gated Ca^{2+} channels (Ca_V) (14, 20, 21). The Ca_V Ca^{2+} influx leads to an increase in intracellular Ca^{2+} concentration that locally triggers insulin vesicle exocytosis (11, 22–27). Concomitantly, Ca^{2+} influx through high-voltage-gated Ca^{2+} channels generates the characteristic Ca_V-dependent β cell electrical activity (12, 14, 28, 29). The glucose-induced electrical activity of the β cells consists of trains of action potentials (APs) superimposed on a depolarizing plateau potential (PP) separated by hyperpolarized silent periods (30, 31). Increasing the extracellular glucose concentration prolongs the AP-train duration, culminating with a continuous firing in glucose concentrations above 15 mM. During the AP train, the firing pattern can be characterized by single APs or bursts of APs (32). The membrane repolarization during an AP and at the end of an AP train is supported by the activation of large-conductance (BK) (33, 34) and small-conductance (SK) Ca^{2+}-activated K^+ channels (35, 36). However, in both mouse (32) and human (37, 38) β cells, the membrane repolarization after an AP is primarily controlled by the activation of the voltage-gated $K_V2.1$ K^+ channels (39). $K_V2.1$ genetic ablation (32) or pharmacological inhibition (37, 40–43) prolongs AP duration and increases the percentage of cells firing AP bursts.

Conflict of interest: The authors have declared that no conflict of interest exists.

Submitted: April 19, 2023
Accepted: February 8, 2024
Published: February 15, 2024

Reference information: *JCI Insight*. 2024;9(6):e171609. https://doi.org/10.1172/jci.insight.171609.

This results in increased cytosolic Ca^{2+} concentration, causing higher insulin release and enhanced glucose tolerance (32, 41, 42). Additionally, $K_V2.1$ can directly increase insulin release independently of its effects on β cell electrical activity by enhancing vesicle recruitment and exocytosis (44–46) as well as promoting β cell survival (43, 47).

Previously, we have shown that female mice have enhanced glucose tolerance compared with males (48). However, this was not caused by sex-specific differences in insulin sensitivity at 4 weeks or pancreatic islet area at 14 weeks. Paradoxically, despite similar β cell Ca_V Ca^{2+} current influx, the glucose-induced islet Ca^{2+} transients were smaller in females compared with males, but caused a significantly higher second-phase insulin release (48).

Here, we aimed to determine whether the higher insulin release from female islets is caused by an enhanced glucose-induced electrical activity, higher intracellular Ca^{2+} amplification, or enhanced insulin granule exocytosis. Mechanistically, our data show that glucose stimulation leads to a higher membrane depolarization and electrical activity in female β cells compared with those of males. The more depolarized MP in female β cells led to reduced Ca_V channel availability, explaining the previously observed smaller glucose-induced islet Ca^{2+} transients (48). The sex-specific difference in β cell MP was caused by approximately 2-fold higher $K_V2.1$ K^+ currents in male compared with female β cells. Despite a different $K_V2.1$ conductance, the insulin granule exocytosis was identical between sexes. Therefore, the smaller $K_V2.1$ K^+ currents promote glucose-induced electrical activity, leading to a larger second-phase insulin release and better glucose tolerance in females.

Results

Female β cells have higher electrical activity compared with those of males. To characterize the glucose-induced electrical activity, we performed patch-clamp experiments in current-clamp mode in β cells still part of the intact pancreatic islet perfused with increasing glucose concentrations in a stepwise manner (2, 5, 7.5, 10, 15, and 20 mM) (Figure 1A). In 2 mM glucose, β cells of both sexes showed no electrical activity and a similar resting MP ($RMP_{females}$ = –65.6 ± 3.1 mV, RMP_{males} = –71.7 ± 2.3 mV; Figure 1, A and B). Increasing the glucose concentration led to an increase in the electrical activity in a concentration-dependent manner in β cells of both sexes. However, the average of the electrical activity shows that only female β cells responded with a steady membrane depolarization (Figure 1A). Sample traces (Supplemental Figure 1; supplemental material available online with this article; https://doi.org/10.1172/jci.insight.171609DS1) show that the MP of male β cells frequently undergoes episodes of hyperpolarization, while in female β cells the MP remains depolarized. Therefore, the average MP will be more hyperpolarized in males compared with female β cells (Figure 1A and Supplemental Figure 1). The most negative MPs (Figure 1B) and PP (Figure 1C) were significantly more depolarized in females compared with males (i.e., in 15 mM glucose, $MP_{females}$ = –50.0 ± 7.1 mV, MP_{males} = –82.7 ± 6.3 mV, $P < 0.001$; $PP_{females}$ = –41.22 ± 7.35 mV, PP_{males} = –74.3 ± 6.8 mV; $P = 0.003$). In addition, the AP-train frequency (f) in 10 mM glucose was significantly higher in female compared with male β cells ($f_{females}$ = 1.76 ± 0.25 trains/min, f_{males} = 1.14 ± 0.15 trains/min; $P = 0.03$) (Figure 1D). Despite the higher AP-train frequency, the fraction of time that a β cell spent in the PP phase (FOPP) at each stimulatory glucose concentration was identical between sexes, demonstrating that the β cells of both sexes have a similar glucose sensitivity (EC_{50} $glucose_{female}$ = 9.45 ± 0.15 mM, EC_{50} $glucose_{male}$ = 9.42 ± 0.16 mM) (Figure 1E). This apparent discrepancy can be reconciled by the observation that in 10 mM glucose, male β cells displayed longer AP trains compared with females ($Duration\text{-}train_{male}$ = 65.5 ± 30.2 seconds, $Duration\text{-}train_{female}$ = 20.3 ± 3.7 seconds; $P = 0.03$) (Figure 1D). The AP firing properties showed many sex-specific differences (Figure 1, F–J). During an AP train, β cells can display 2 different firing patterns: single AP firing and AP bursts (Figure 1F). In 7.5 and 10 mM extracellular glucose, females had a higher percentage of cells showing burst firing mode compared with males. In 10 mM glucose, 25% of the cells from males show only single AP firing, while in females 100% of the cells showed a mixed firing pattern of both single APs and AP bursts (Figure 1G). While the AP or AP-burst frequency and amplitude (Figure 1I) were not significantly different between sexes in most glucose concentrations, the AP frequency in 7.5 mM glucose (Figure 1H) (f_{males} = 3.5 ± 0.5 Hz, $f_{females}$ = 6.2 ± 0.8 Hz; $P = 0.0086$) and the AP-burst duration (Figure 1J) were almost double in females compared with males (in 10 mM glucose, $Burst\text{-}duration_{females}$ = 0.42 ± 0.06 seconds and $Burst\text{-}duration_{males}$ = 0.24 ± 0.03 seconds; $P = 0.04$). These results demonstrate that the glucose-induced electrical activity is higher in females compared with males as a result of a higher frequency of AP trains and higher AP firing frequency at lower glucose concentration, higher incidence of AP bursts, and longer AP-burst duration.

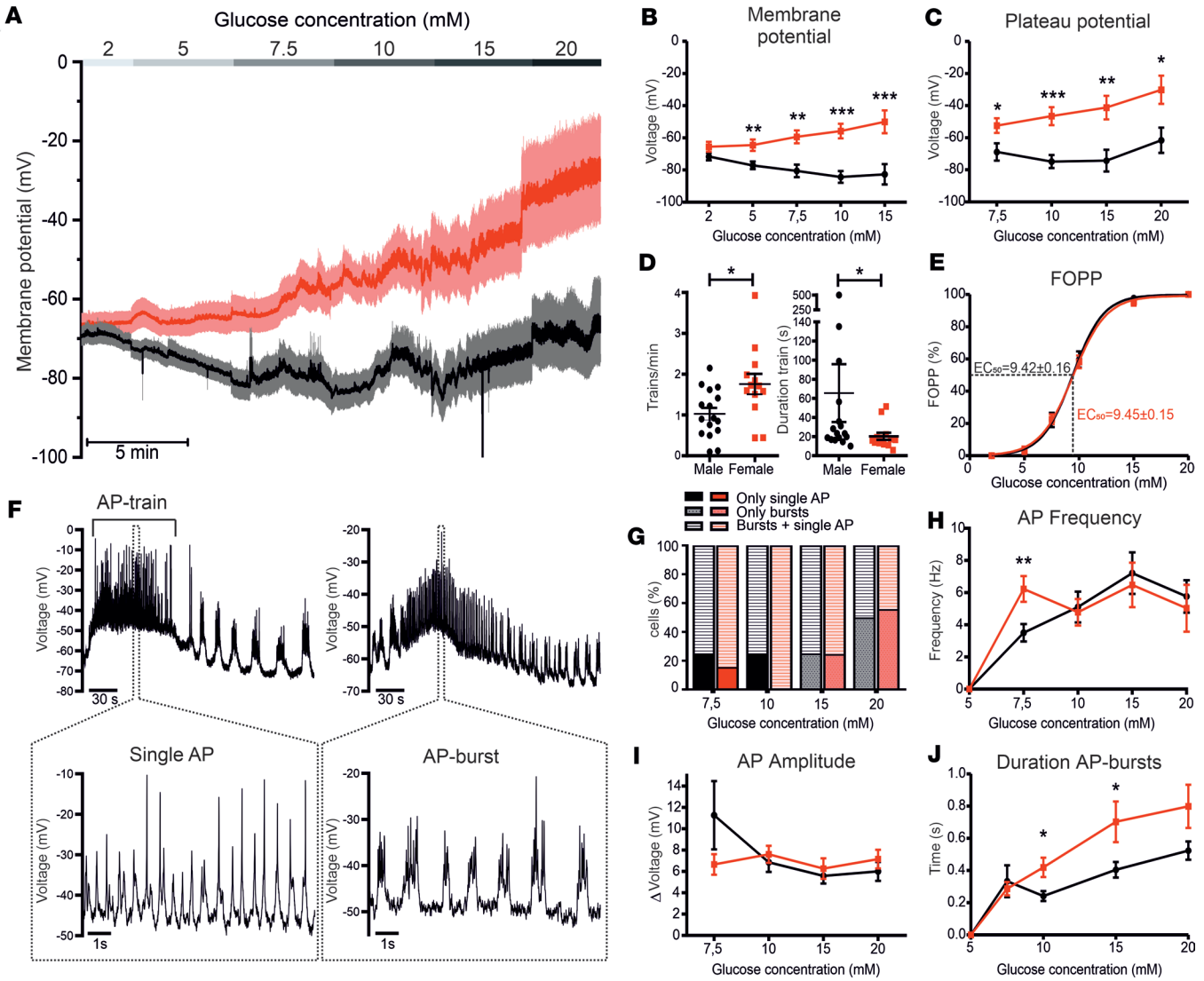

Figure 1. Female β cells show a more depolarized MP and PP and higher electrical activity in all stimulatory glucose concentrations compared with male β cells. (**A**) Average traces of the glucose-induced electrical activity in male (black, *n* = 10–20; 8 mice) and female β cells (red, *n* = 11–14; 6 mice) stimulated with 2, 5, 7.5, 10, 15, and 20 mM glucose. Female β cells show a significantly more depolarized MP (**B**) and PP (**C**). (**D**) AP-train frequency in 10 mM glucose was significantly higher in female β cells, while the duration of the AP trains was significantly longer in males. This leads to a similar fraction of plateau phase (FOPP) and glucose sensitivity (EC_{50}) (**E**). (**F**) Sample traces of characteristic β cell electrical activity showing single-AP-firing mode (left) and AP-burst mode (right). (**G**) Percentage of cells showing the different firing patterns induced by different glucose concentrations from male (black) and female (red) β cells. Single AP firing is shown in dark colors, AP burst is shown in gray and light red, while mixed firing is represented by the striped pattern. (**H**) Frequency and (**I**) amplitude of APs in male and female β cells in different glucose concentrations. (**J**) AP-burst duration is longer in females in 10 and 15 mM glucose. All values are mean ± SEM. **P* < 0.05, ***P* < 0.01, ****P* < 0.001 by 2-tailed Student's *t* test.

K_{ATP} and K_2P currents do not differ between sexes. K_{ATP} channel activity is responsible for maintaining the pancreatic β cells' hyperpolarized RMP under low extracellular glucose levels (15, 16). To investigate whether the higher glucose-induced membrane depolarization in female β cells is caused by different K_{ATP} channel expression or activation, we measured the K^+ currents (IK) using a ±10 mV square pulse protocol from a holding potential of –70 mV (Figure 2A). The average traces of K_{ATP} current densities in the presence of 2 mM extracellular glucose and 340 μM diazoxide, a K_{ATP} channel activator that works independently of the ATP/ADP ratio, showed no sex difference (i.e., in 2 mM glucose and at –60 mV $IK_{ATP\text{-}male}$ = 6.47 ± 1.12 pA/pF, $IK_{ATP\text{-}female}$ = 6.45 ± 0.8 pA/pF; *P* = 0.98) (Figure 2, A and C). Considering that in 5 mM glucose the β cell MP was significantly different between sexes (Figure 1B), we asked whether the K_{ATP} channel endogenous inhibition is sex specific. When measured in 5 mM glucose, the K_{ATP} currents were also similar in the β cells of both sexes at both tested MPs (i.e., in 5 mM glucose and at –60 mV $IK_{ATP\text{-}male}$ = 2.17 ± 0.41

pA/pF, $IK_{ATP\text{-}female}$ = 1.98 ± 0.43 pA/pF; P = 0.74) (Figure 2, B and D). Together, these results demonstrate that the K_{ATP} channel expression or inhibition in pancreatic β cells is not sex specific. Other potential targets involved in maintaining the MP and PP in high glucose concentrations are the K_2P channels TASK-1 and TALK-1 (18, 19). However, a 1-second-long ramp protocol from –120 mV to +60 mV (Figure 2E) elicited similar K^+ current densities in β cells of both sexes (i.e., at –120 mV IK_2P_{male} = –7.32 ± 1.7 pA/pF; IK_2P_{female} = –6.41 ± 0.61 pA/pF) (Figure 2, E and F), thus excluding their involvement in the sex-specific β cell MP.

β Cell–induced electrical activity is similar between sexes. The different MPs alone could be responsible for all observed sex-specific differences in AP frequency and AP-burst duration (Figure 1). To test this hypothesis, we measured the induced electrical activity in response to stepped-current injections in single isolated pancreatic β cells. For this, we clamped the β cell MP at –80 mV and induced depolarizations using 2-second-long current injections in 2-pA increments (Figure 3A). The minimal current injected to elicit AP firing, also referred as rheobase, was similar between β cells of both sexes (Figure 3B). Similarly, the number of APs recorded at rheobase, the PP and AP threshold potential, as well as AP amplitude, time to peak, and the 50% of the maximal AP amplitude did not show any sex difference (Figure 3, C–H). These observations demonstrate that the sex difference in AP frequency and AP-burst duration were largely caused by the altered MP. However, male β cells take significantly longer time to reach the AP depolarization threshold (t_{males}= 0.97 ± 0.08 seconds, $t_{females}$ = 0.63 ± 0.07 seconds; P = 0.0035) (Figure 3I) and the after-hyperpolarization (AHP) amplitude was larger in females compared with males (AHP_{males} = 2.04 ± 0.70 mV, $AHP_{females}$ = 4.43 ± 0.56 mV; P = 0.0126) (Figure 3J), indicating possible sex-specific differences in β cell voltage-gated (K_v) and Ca^{2+}-activated K^+ currents.

The Ca^{2+}-activated K^+ current amplitudes are similar between sexes but show different kinetics and Ca^{2+} dependence. In pancreatic β cells, Ca^{2+}-activated BK and SK K^+ channels contribute to AP repolarization and shape (34, 49–54). To characterize the BK and SK channel Ca^{2+} dependence, we used a double-pulse protocol consisting of a variable-length prepulse to 0 mV in 90-ms increments that opens the Ca_Vs, thus progressively loading the cell with Ca^{2+}, followed by a test pulse to +80 mV that activates the BK and SK currents (Figure 4A). The BK and SK components were isolated by subtracting the currents in the presence of 1 μM paxilline and 200 nM apamin from the total K^+ currents. The maximal BK current amplitudes (Figure 4D) did not differ between male (Figure 4B) and female β cells (Figure 4C). However, the BK current decay was significantly faster in females if the Ca^{2+} loading prepulse was shorter than 0.8 seconds (Figure 4, G–I). Following a Ca^{2+} loading prepulse of 90 ms, the remaining current after a 500-ms test pulse was approximately 1.5-fold higher in males compared with females (I_{BK}-$R_{500male}$ = 66.8% ± 6.81%, I_{BK}-$R_{500female}$ = 43.55% ± 8.12%; P = 0.04) (Figure 4, G and I). After the application of 200 nM apamin, the calculated SK current component was significantly higher in females compared with males only if the Ca^{2+} preloading step was 90 ms long (I_{SKmale} = 47.08 ± 17.06, $I_{SKfemale}$ = 161.88 ± 51.67; P = 0.037) (Figure 4, D and F). Together, these results demonstrate a different contribution of BK and SK K^+ currents to β cell membrane repolarization during an AP at low-frequency electrical activity, explaining the observed higher AHP component in female β cells compared with males (Figure 3J). However, during the repetitive firing of an AP train, simulated in our protocol by longer Ca^{2+} preloading steps, the contribution of BK and SK to β cell electrical activity will be similar in both sexes. Interestingly, the remaining voltage-gated K^+ currents after the addition of both 1 μM paxilline and 200 nM apamin were significantly higher in males compared with females (IK_{Vmales} = 1015.25 ± 121.59 pA, $IK_{Vfemales}$ = 694.25 ± 58.07 pA; P = 0.016) (Figure 4, E and F).

Male β cells have larger K_v2.1 currents that set the MP. To investigate whether this observed change in the K^+ current amplitude is also associated with a sex-specific modulation of K_v channel voltage dependence of activation and inactivation, we used a 3-pulse protocol (55) consisting of 2 test pulses 300 ms long to +60 mV (P_1 and P_3) separated by a 15-second-long conditioning pulse (P_2) from –100 mV to +60 mV in 20-mV increments (Figure 5A). The voltage dependence of activation was determined using the maximal amplitude during the conditioning P_2 pulse, while the voltage dependence of inactivation was measured using the maximal amplitude of the last P_3 test pulse in comparison with the P_1 pulse. The conditioning pulse elicited significantly higher K^+ currents in male β cells compared with females at membrane depolarization above 0 mV (at +60 mV, IK_{Vmales} = 149 ± 24.1 pA/pF; $IK_{Vfemales}$ = 82.3 ± 13.3 pA/pF; P = 0.0269) (Figure 5B). Nevertheless, the voltage dependence of activation and inactivation (Figure 5C) as well as the percentage of inactivation (data not shown) remained similar between β cells of both sexes. β Cells express several K_v channel isoforms, with K_v2.1 conducting approximately 70% of the total K_v currents (32, 37, 38, 56). To investigate whether the observed sex difference in K_v current amplitude is caused by different K_v2.1 conductance, we measured the

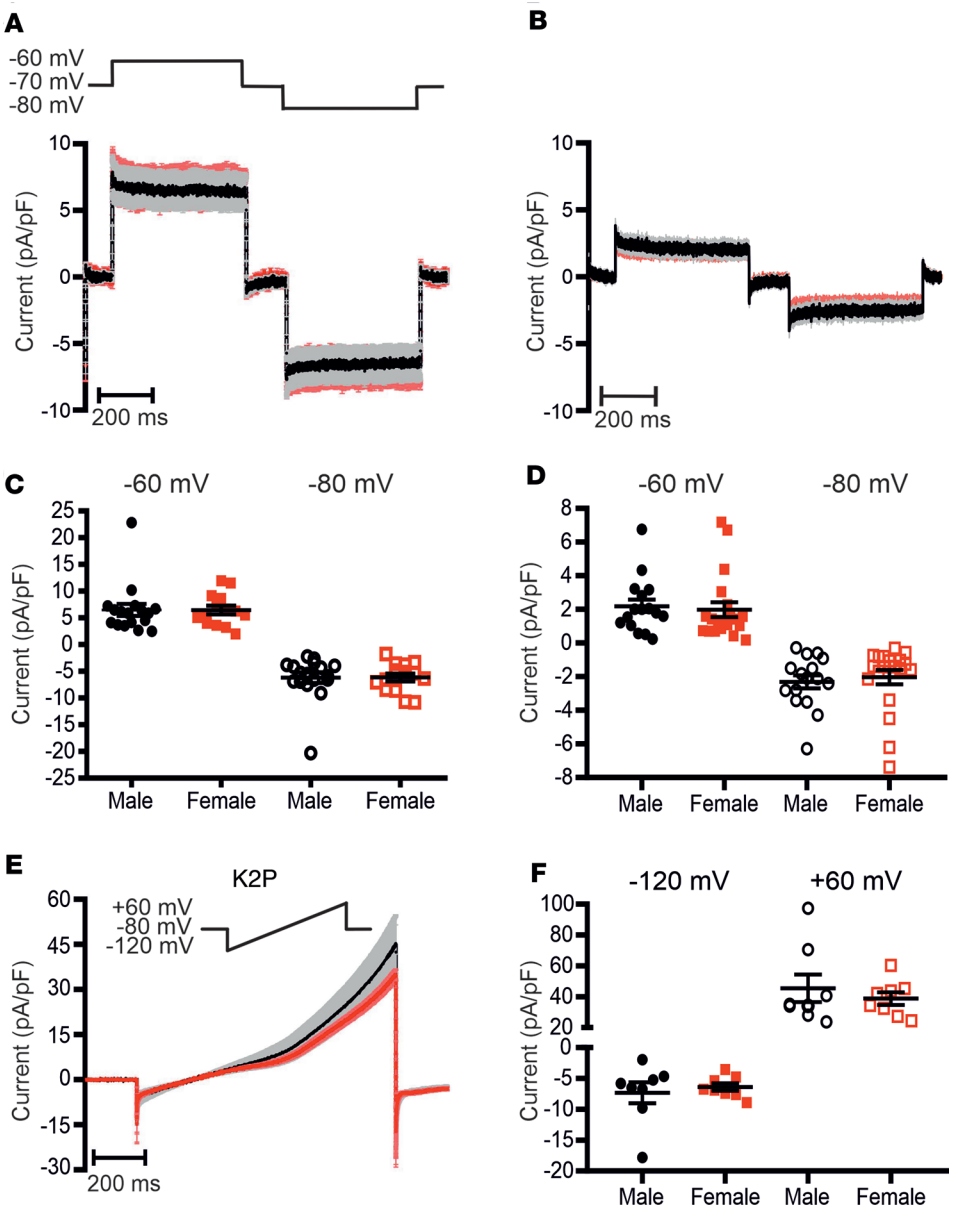

Figure 2. K_{ATP} and TASK/TALK currents do not differ between β cells of both sexes. (**A**) Average traces of males (black, *n* = 17; 3 mice) and female (red, *n* = 15; 3 mice) K_{ATP} current in the presence of 2 mM glucose and 340 mM diazoxide (Dzx). (**B**) K_{ATP} currents in the presence of 5 mM extracellular glucose. (**C**) K_{ATP} current density at –60 mV (filled symbols) and –80 mV (empty symbols) in the presence of 2 mM glucose plus 340 mM Dzx. (**D**) K_{ATP} current density at –60 mV (filled symbols) and –80 mV (empty symbols) in the presence of 5 mM glucose. (**E**) One-second ramp protocol used to record the K_2P currents from –120 mV to +60 mV (top) and average traces of K_2P current recorded in male (black, *n* = 8; 3 mice) and female (red, *n* = 8; 3 mice) β cells. (**F**) K_2P current densities at –120 mV (filled symbols) and at +60 mV (empty symbols) in β cells of both sexes. All values are mean ± SEM. Significance was evaluated by 2-tailed Student's *t* test.

total K^+ current in the absence and presence of the specific $K_v2.1$ blocker stromatoxin-1 (Strx-1, 100 nM) using a 500-ms-step depolarization pulse from –80 mV to +80 mV in 10-mV increments (Figure 5, D and G). Male β cells had significantly higher total K^+ current density (Figure 5, E and F) compared with females (IK_{Vmales} = 166.97 ± 8.97 pA/pF, $IK_{Vfemales}$ = 126.1 ± 11.3 pA/pF; P = 0.0135). The remaining K^+ current after the addition of 100 nM Strx-1 was similar in β cells of both sexes, demonstrating that only $K_v2.1$ conductance is sex specific (Figure 5, E and F). Calculating the Strx-1–sensitive component by subtraction showed that male β cells conduct approximately 1.7-fold higher $K_v2.1$ currents compared with females ($IK_v2.1_{males}$ = 131.15 ± 6.79 pA/pF, $IK_v2.1_{females}$ = 75.8 ± 11.34 pA/pF; $P < 0.001$) (Figure 5, H and I), with a similar

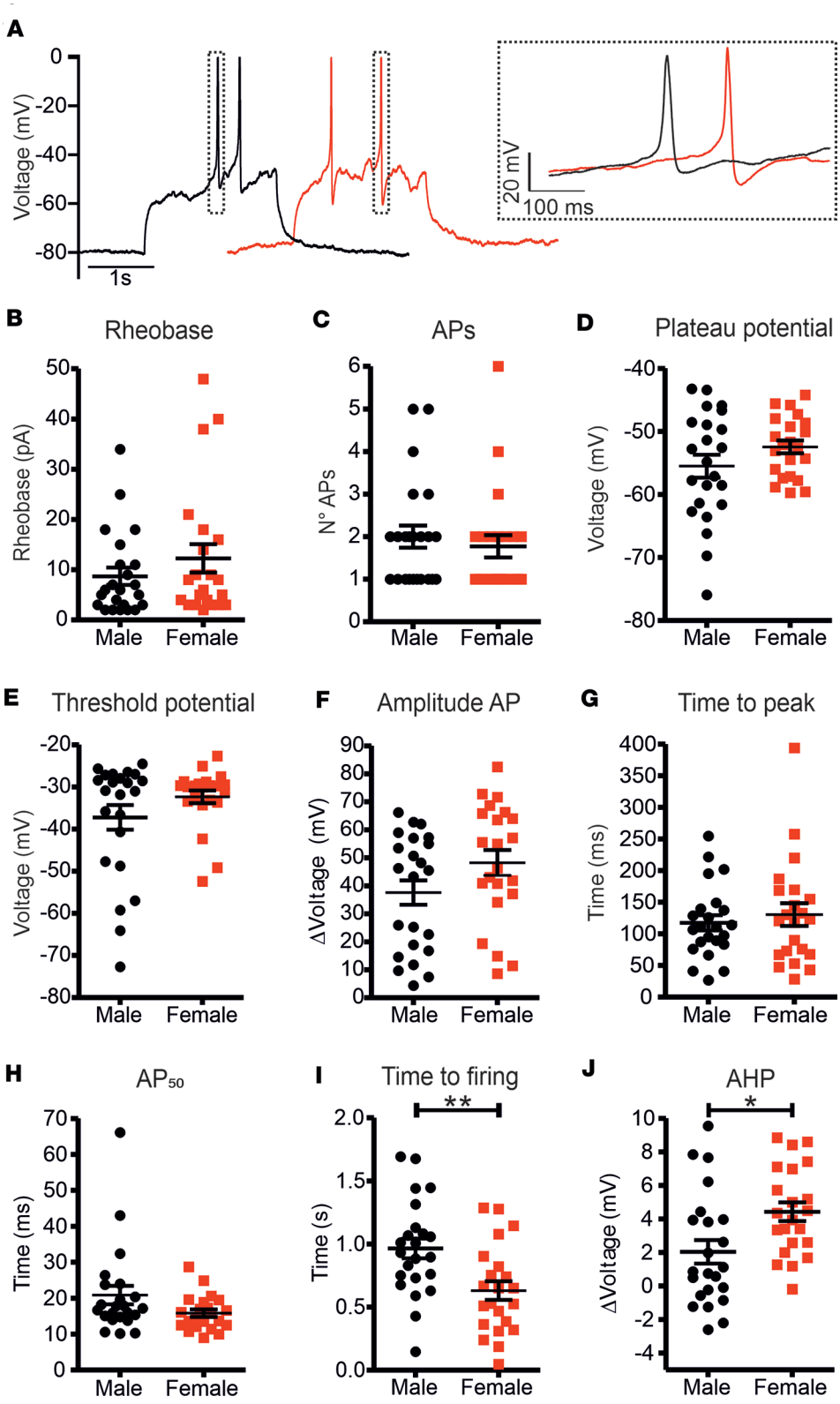

Figure 3. Induced electrical activity in isolated β cells from male and female mice. (**A**) Sample traces of the induced electrical activity recorded at the rheobase current injection from both male (black, *n* = 23; 3 mice) and female (red, *n* = 21; 3 mice) isolated β cells. The rheobase was not significantly different between males and females (**B**) and neither was the number of APs (**C**). Both the plateau potential (**D**) and the threshold potential of the AP upstroke phase (**E**) were not significantly different, nor were the AP amplitude (**F**), time to peak (**G**), and 50% of the maximal amplitude (AP_{50}) (**H**). The time to firing of the first AP (**I**) was significantly longer in male β cells, while the AP after hyperpolarization (AHP) component (**J**) was significantly higher in female β cells compared with males. All the parameters shown are calculated from the first AP at the rheobase. All values are mean ± SEM. $^{*}P < 0.05$, $^{**}P < 0.01$ by 2-tailed Student's *t* test.

voltage dependence of activation (Figure 5H, inset). Together, these results suggest that the different $K_v2.1$ conductance accounts for the observed sex-specific difference in MP. However, this is in divergence with the known role of $K_v2.1$ channels as delayed rectifier channels responsible for membrane repolarization during an AP. To investigate whether the MP is modulated by $K_v2.1$, we measured the glucose-induced electrical activity in male β cells without any drug application and subsequently in the presence of 100 nM Strx-1 (Figure 5J).

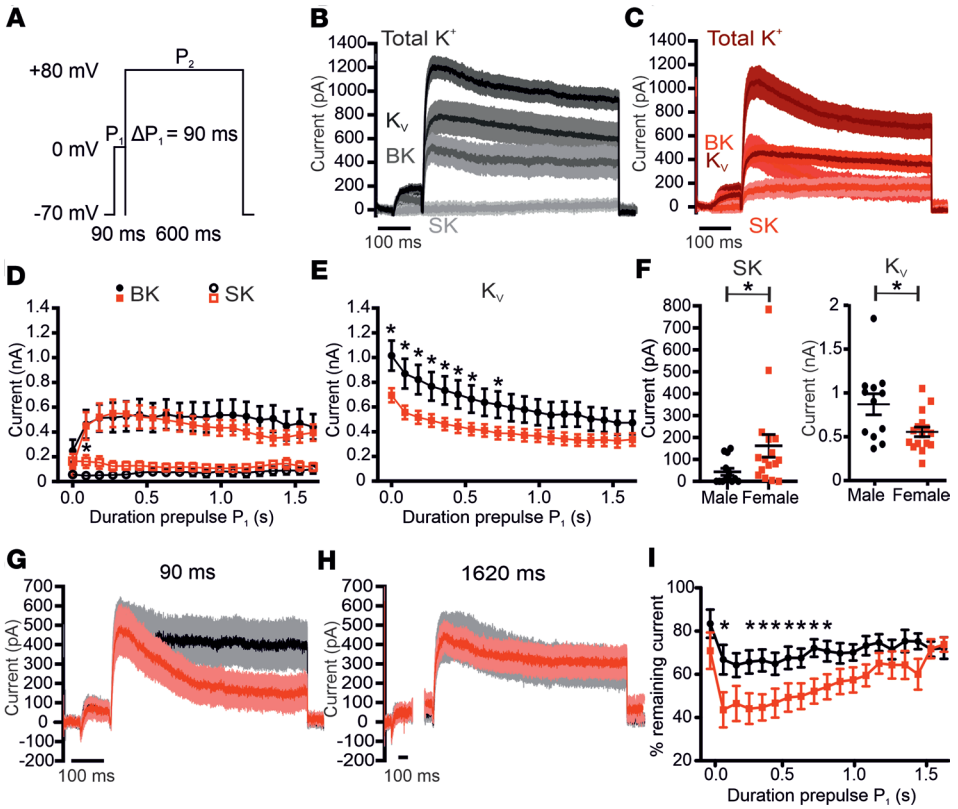

Figure 4. Ca^{2+}-activated K^+ current amplitude is similar in β cells of both sexes but shows different kinetics and Ca^{2+} dependence. (**A**) Protocol used for measuring Ca^{2+}-activated K^+ current, which consisted of a variable-length Ca^{2+}-loading prepulse to 0 mV (P_1), with each sweep increasing in length by 90 ms, followed by a test pulse (P_2) to +80 mV to measure K^+ currents. (**B** and **C**) Average trace of total, BK, SK, and K_v currents from male (n = 12; 3 mice) (**B**) and female (n = 16; 4 mice) (**C**) β cells at P_1 = 90 ms. (**D**) The BK (full symbols) and SK (empty symbols) current components were obtained by subtraction from the total K^+ current after the sequential addition of 1 μM paxilline and 200 nM apamin. (**E**) The remaining current after BK and SK block represents the K_v current component. (**F**) Scatter plot showing the significantly higher SK (left) and K_v currents (right) at P_1 = 90 ms. (**G**) The BK current kinetics following a P_1 = 90 ms or (**H**) P_1 = 1620 ms prepulse recorded in male and female β cells. (**I**) The remaining BK current at the end of the 600 ms P_2 pulse is significantly larger in male β cells compared with females if the P_1 prepulse is shorter than 800 ms. All values are mean ± SEM. *P < 0.05 by Mann-Whitney test (**D** and **F**) or 2-tailed Student's t test (**E**, **F**, and **I**).

As shown in Figure 1, increasing the glucose concentration in male β cells from 2 to 5 and 7.5 mM did not result in an MP depolarization even after a continuous 30-minute application (Supplemental Figure 1). Nevertheless, the addition of 100 nM Strx-1 significantly depolarized the MP by approximately 20 mV (Figure 5, J and K, and Supplemental Figure 1). These results demonstrate what we believe is a novel role for K_v2.1 in maintaining the β cells' MP. Additionally, a different K_v2.1 expression or localization could lead to a sex-specific insulin release independently of its ion-conducting pore function. Overexpression of a K_v2.1 pore mutant channel increased vesicle exocytosis (44), while K_v2.1 silencing resulted in impaired exocytosis due to reduced vesicle recruitment and fusion (45, 46). Therefore, a potentially reduced K_v2.1 channel expression in female β cells might result in impaired vesicle exocytosis. Conversely, our previous report showing a higher insulin secretion and better glucose tolerance in females (48) might indicate more exocytosis from female β cells.

Vesicle exocytosis is similar in β cells of both sexes, but the incretin pathway is different. Insulin vesicle fusion with the plasma membrane increases the cell surface that can be measured as an increase in cell capacitance (Cm). In response to a train of 10 depolarizing steps 500 ms long to 0 mV that activates the Ca_V Ca^{2+} influx, the total increase in Cm was identical between β cells of both sexes (Figure 6, A and B). Following the first depolarization step, the initial Cm increase is a direct measurement of the already primed, readily releasable pool (RRP) of vesicles (Figure 6B). The β cells of both sexes did not show any difference either in the first or in the subsequent steps (Figure 6, A and B). Previously, it has been demonstrated that K_v2.1 pharmacological inhibition (37, 42, 43) or genetic ablation (32) enhanced both phases of insulin release (42). However, consistent with our

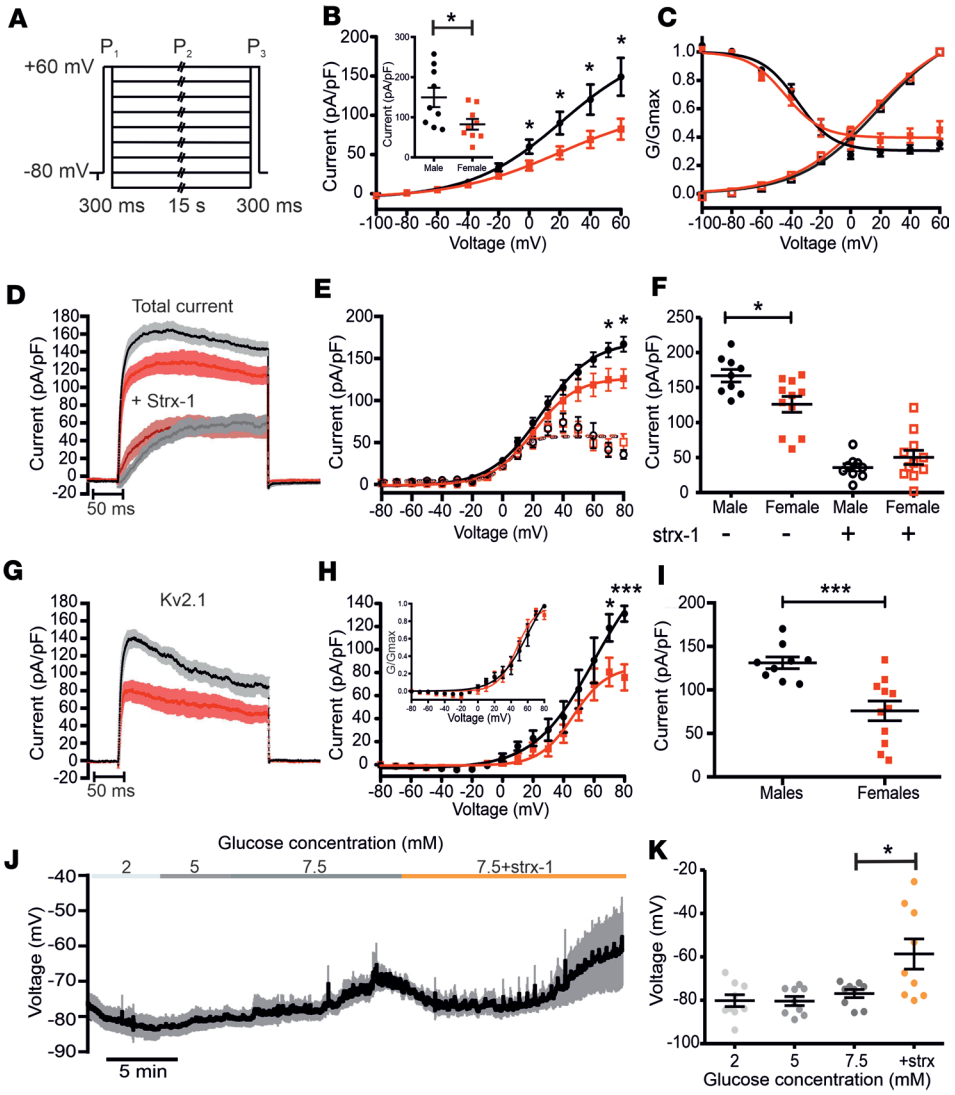

Figure 5. K_v2.1 current density is higher in males compared with females and it modulates the MP. (**A**) The 3-pulse protocol used to characterize the voltage sensitivity of the K_v channel activation and inactivation. (**B**) The current density amplitude was significantly higher in males (black, n = 9; 3 mice) compared with females (red, n = 9; 3 mice). Inset showing the scatter plot of the K_v current density at +60 mV. (**C**) The K_v current voltage dependence of activation (empty symbols) and inactivation (full symbols) were not different between β cells of male and female mice. (**D**) Average trace of the K^+ current measured in males (n = 9; 3 mice) and female (n = 9; 3 mice) in the absence or presence of 100 nM specific K_v2.1 blocker stromatoxin-1 (Strx-1) (males in gray; females in wine). (**E**) K^+ current-voltage relationship without Strx-1 (full symbols) and after the addition of Strx-1 (empty symbols) in pancreatic β cells of both sexes. (**F**) Scatter plot showing the individual values of the K^+ currents with and without Strx-1 in both male and female β cells at +80 mV. (**G**) Average trace of Strx-1–sensitive K_v2.1 K^+ currents calculated by subtraction from panel **D**. (**H**) Current-voltage relationship of K_v2.1 currents. Inset shows the normalized conductance. (**I**) Scatter plot of the K_v2.1 current density at +80 mV. (**J**) Average of glucose-induced electrical activity of male β cells (n = 9; 3 mice) in intact islets with and without 100 nM Strx-1. (**K**) Scatter plot of the the average MP in male β cells with and without 100 nM Strx-1. All values are mean ± SEM. $^*P < 0.05$; $^{***}P < 0.001$ by paired or unpaired, 2-tailed Student's t test.

previous report (48) and the Cm measurements, the first phase of insulin release did not show any significant sex-specific difference (Figure 6C). Partial K_v2.1 current inhibition has also been shown to enhance glucagon-like peptide-1 (GLP-1) receptor activation insulinotropic effects, but only at subthreshold exendin-4 levels and not maximal activation (42). Consistent with this observation, maximal receptor activation with 1 nM GLP-1 resulted in the same augmentation of insulin release in β cells of both sexes (Figure 6D). Nevertheless, recently it has been reported that chronically depolarized β cell MP alters the GLP-1 receptor downstream signaling cascade, showing a higher contribution of the G_q pathway compared with G_s (57). Consistent with this

notion and the more depolarized MP in female β cells (Figure 1), the application of 100 nM YM-254890, a G_q pathway inhibitor, in parallel with 1 nM GLP-1 resulted in a significantly greater inhibition of insulin release from female islets compared with male islets (Insulin $peak_{males}$ = 33.9 ± 9.5 pg/min/islet, Insulin $peak_{females}$ = 14.75 ± 3.03 pg/min/islet; P = 0.04) (Figure 6, E and F). Importantly, the application of 100 nM YM-254890 alone in the absence of GLP-1 stimulation led to a similar, nonsignificant reduction in peak insulin release in islets of both sexes (Supplemental Figure 2), demonstrating that the basal G_q pathway activation does not show a sex difference. Together, these results demonstrate that neither insulin vesicle priming and release nor maximal incretin effects are sex specific. This indicates that the previously reported higher second-phase insulin release in female islets could be caused by the increased electrical activity alone. However, contradicting this notion is the observation that the glucose-induced islet Ca^{2+} transients were smaller in females compared with males, despite similar Ca_V Ca^{2+} current density (48).

Different MP alters the Ca_V channel availability. The smaller islet Ca^{2+} transients despite similar Ca^{2+} influx could be a consequence of reduced intracellular Ca^{2+}-store filling and release. To test this hypothesis, we measured the endoplasmic reticulum (ER) intracellular store Ca^{2+} release by activation of the inositol 1,4,5-trisphosphate (IP_3) receptors (IP_3Rs) with 200 nM carbachol (Cch) (Figure 7A). To exclude the contribution of Ca^{2+} influx to cytosolic Ca^{2+} concentration, the islets were bathed in an extracellular solution containing 0 mM Ca^{2+}. The peak amplitude of ER Ca^{2+} release had the same amplitude in islets of both sexes (Figure 7, A and B); however, the time to peak of Ca^{2+} transients in female islets was significantly slower ($CchTtp_{male}$ = 5.21 ± 0.17 seconds, $CchTtp_{females}$ = 7.89 ± 0.52 seconds; P < 0.001). ER-store depletion activates the β cell store–operated Ca^{2+} entry (SOCE) (58, 59). Following perfusion with physiological solution containing 2.5 mM Ca^{2+}, the islets of both sexes showed similar SOCE amplitude and kinetics (Figure 7C). If Ca_V Ca^{2+} influx density (48), intracellular Ca^{2+} store release, and ER-depletion-triggered SOCE are similar, then how could the islet Ca^{2+} transients be reduced in female islets (48) compared with males? Upon membrane depolarization, most Ca_V channel isoforms undergo time-dependent conformational rearrangements that drive the channel into an inactivated state (14). To test the effect of the sex-specific difference in MP (Figure 1B) on Ca_V availability, we measured the Ca^{2+} current density in male and female β cells starting from an MP of –80 mV, corresponding to the male β cells (Figure 7D), or –50 mV (Figure 7E), corresponding to the measured MP in female β cells stimulated with 15 mM glucose (Figure 1B). Confirming our previous report (48), Ca^{2+} influx in β cells of both sexes had a similar amplitude and voltage dependence if the MP is identical (Figure 7, F–I). However, if the MP is maintained at –50 mV, then the Ca^{2+} current amplitude in β cells of both sexes decreases by approximately 60% (Figure 7, F and G) (Males: $Imax_{-80mV}$ = –7.3 ± 0.83 pA/pF, $Imax_{-50mV}$ = –2.88 ± 0.7 pA/pF; P < 0.001. Females: $Imax_{-80mV}$ = –7.34 ± 1.3 pA/pF, $Imax_{-50mV}$ = –2.84 ± 0.85 pA/pF; P = 0.011). Additionally, the voltage dependence of activation was shifted toward higher potentials by approximately 10 mV (Figure 7, H and I) (Males: $Vhalf_{-80mV}$ = –19 ± 0.98 mV, $Vhalf_{-50mV}$ = –9.2 ± 2.8 mV; P = 0.01. Females: $Vhalf_{-80mV}$ = –16.09 ± 2.0 mV, $Vhalf_{-50mV}$ = –5.3 ± 1.8 mV; P = 0.0012). Therefore, the increased MP in female β cells reduces the Ca_V channel availability, resulting in smaller Ca^{2+} influx compared with male β cells. Consequently, the reduced Ca^{2+} influx will lead to a smaller amplitude of glucose-induced Ca^{2+} transients in female islets compared with male islets.

Discussion

In humans, the prevalence of diabetes shows a clear sexual dimorphism, with males being more affected compared with females (1–4, 60–65). While peripheral insulin sensitivity is a contributing factor, sex-specific differences in β cell insulin release could also be a strong determinant. Previously, we reported that following an intraperitoneal glucose tolerance test female mice have a significantly higher second-phase insulin release compared with males (48). Paradoxically, the glucose-induced Ca^{2+} transients were significantly smaller in females, while the Ca^{2+} current densities remained unaltered between sexes. Here, we show that a higher glucose-induced membrane depolarization and electrical activity is responsible for this phenomenon in female β cells compared with those of males. Surprisingly, the more depolarized MP in female β cells is not caused by sex-specific K_{ATP} or K_2P channel activity, but significantly reduced $K_V2.1$ channel conductance. Previously, it has been proposed that K^+ efflux mediated by the $K_V2.1$ delayed rectifier channel determines the AP repolarization phase (37, 39, 56, 66). Consequently, $K_V2.1$ genetic ablation in pancreatic β cells increased the AP duration (32). In line with these observations, our data show that female β cells

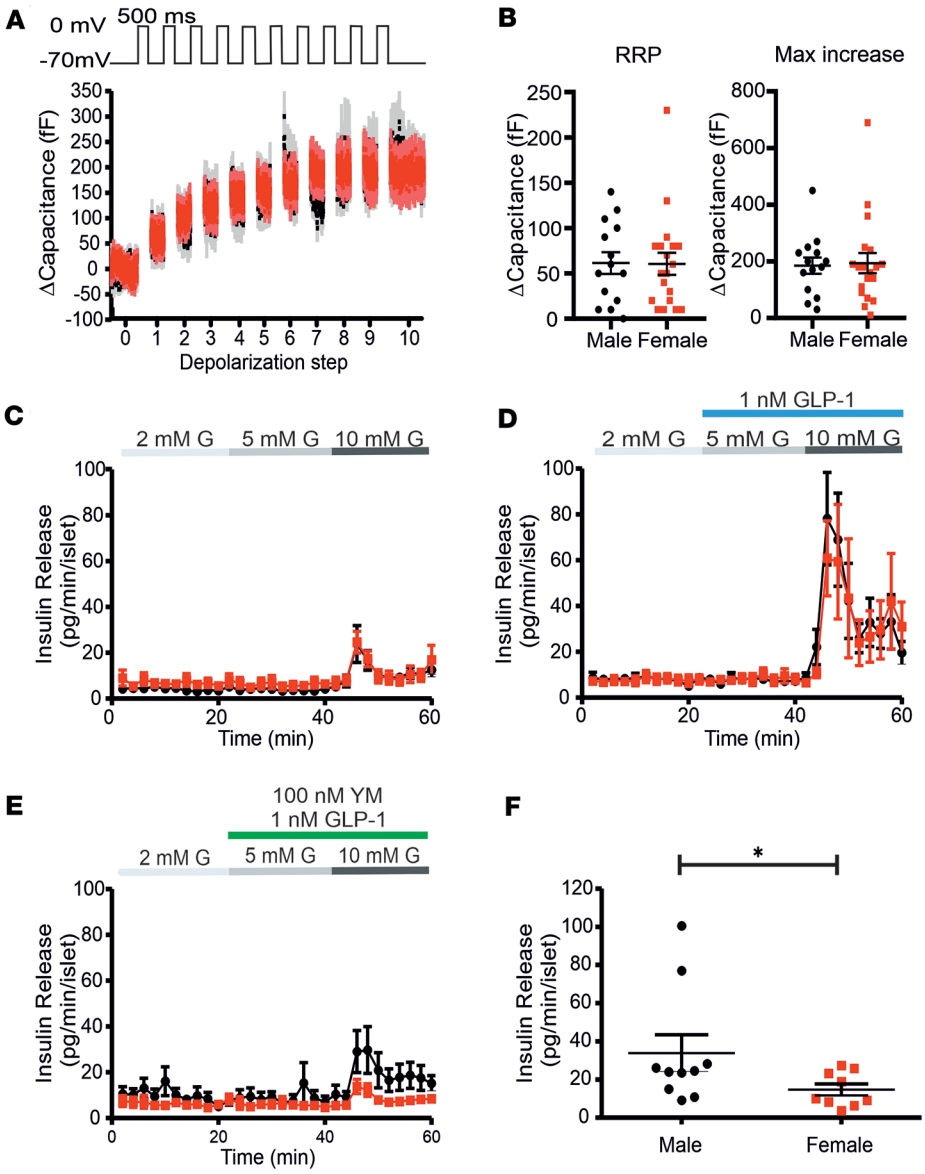

Figure 6. Vesicle exocytosis is similar in male and female β cells, but the incretin pathway shows a sex difference. (**A**) Average trace of the β cell capacitance increase after a train of 10 depolarizing steps (500-ms steps from –70 mV to 0 mV) from male (black, *n* = 15; 3 mice) and female (red, *n* = 19; 3 mice) mice. (**B**) Scatter plot of the increase in capacitance after the first depolarization, corresponding to the readily releasable pool (RRP, left) and the maximal exocytosis (right). (**C**) Dynamic insulin release from male (*n* = 10) and female (*n* = 9) islets (20 islets/experiment) in 2, 5, and 10 mM glucose (**G**). (**D**) Same as in **A** but in the presence of 1 nM GLP-1. (**E**) Dynamic insulin release in 2, 5, and 10 mM glucose plus 1 nM GLP-1 and 100 nM G_q inhibitor YM-254890. (**F**) Scatter plot of the peak insulin release in the presence of 10 mM glucose, 1 nM GLP-1, and 100 nM YM-254890. All values are mean ± SEM. *$P < 0.05$ by 2-tailed Student's *t* test or Mann-Whitney test (**F**).

display longer AP duration manifested as an increase in the percentage of cells showing AP bursts as well as longer AP-burst duration. However, a contradictory finding seems to be that the reduced $K_V2.1$ currents in female β cells stimulated with 7.5 mM extracellular glucose resulted in an increased AP frequency, but $K_V2.1$ genetic deletion resulted in a reduced AP firing frequency (32). These $K_V2.1^{-/-}$ β cells showed a reduced membrane repolarization that is bound to decrease the Ca_V and Na_V channel availability, thus reducing the firing frequency (32). In our experiments, the $K_V2.1$ current density was only partially reduced in female β cells, resulting in a stronger glucose-induced membrane depolarization that sets the PP in the range of the L-type Ca^{2+} channel activation threshold, thus increasing the firing frequency.

The higher electrical activity and reduced $K_V2.1$ currents not only increase insulin release, but also promote β cell survival. $K_V2.1$ overexpression in the INS-1 β cell line activated mitochondrial and ER

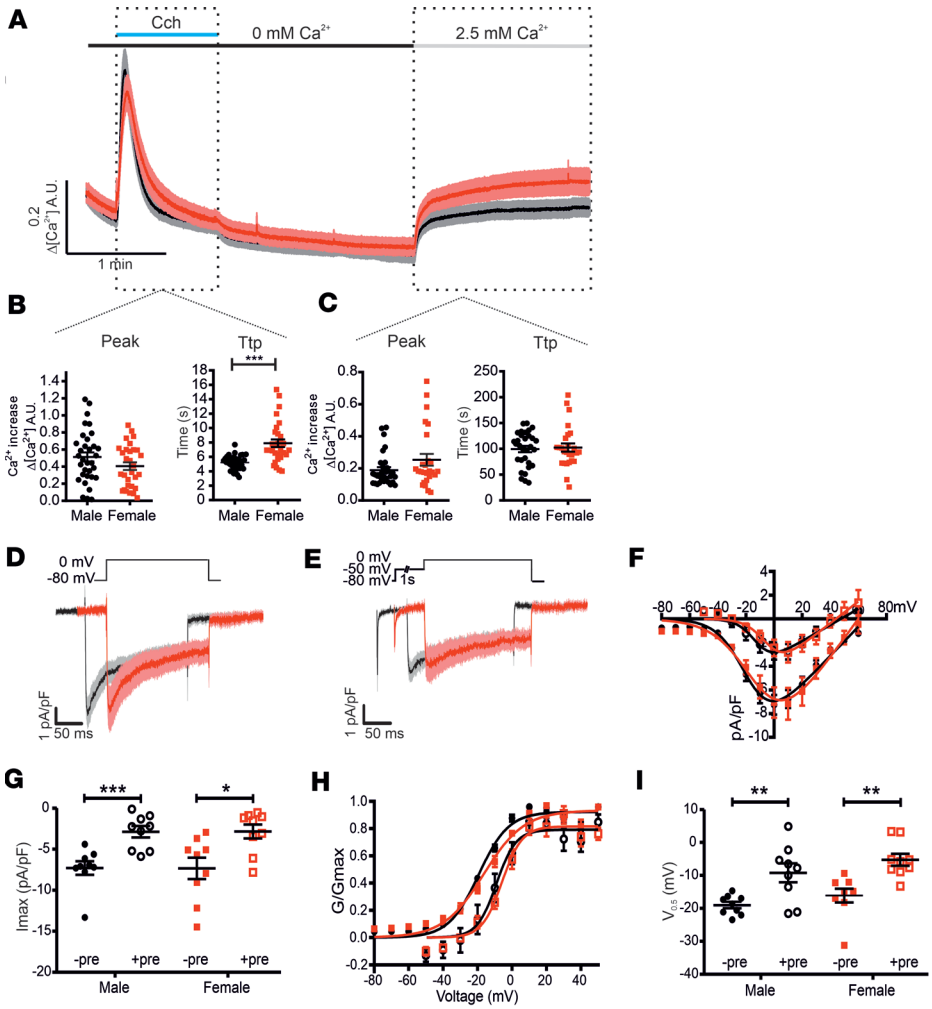

Figure 7. Increased MP reduces the HVCC availability. (**A**) Average Ca^{2+} transients in islets of male (black, *n* = 31–33; 3 mice) and female mice (red, *n* = 26–30; 3 mice). Cch, carbachol. (**B**) Peak amplitude and time to peak (TTP) of Ca^{2+}-store release induced by 0.2 mM carbachol in the presence of 2.5 mM extracellular Ca^{2+}. (**C**) SOCE Ca^{2+} transients measured upon perfusion with 2.5 mM Ca^{2+}–containing solution. (**D**) Average trace of the Ca^{2+} influx in male (black, *n* = 9; 3 mice) and female (red, *n* = 9; 3 mice) β cells from a holding potential of –80 mV or (**E**) after a 1-second-long prepulse to –50 mV. (**F**) The I/V curve and scatter plot of the maximum Ca^{2+} current density (**G**) showing that the prepulse to –50 mV induces a reduction in the Ca^{2+} influx by approximately 60% in both male and female β cells. (**H**) The prepulse to –50 mV shifts the voltage dependence of Ca^{2+} conductance by 10 mV toward more depolarized potentials. (**I**) Scatter plot of half maximal activation values ($V_{0.5}$). All values are mean ± SEM. $^*P < 0.05$; $^{**}P < 0.01$; $^{***}P < 0.001$ by 2-tailed Student's *t* test.

stress–induced apoptosis (47). Consistent with this observation, it has been shown that $K_V2.1$ pharmacological inhibition increases serum insulin levels, restores β cell mass, and decreases fasting blood glucose in a diabetes mouse model (43). The effects could be mediated via an enhanced electrical activity–dependent metabolic memory (67, 68) or alternatively via a reduced Ca^{2+} toxicity. Supporting this notion comes the observation that the more depolarized MP in female β cells causes a significantly reduced Ca_V channel availability and Ca^{2+} influx and therefore reduced glucose-induced islet Ca^{2+} transient amplitude (48). In contrast, the larger $K_V2.1$ current in male β cells causes a hyperpolarized PP, leading to higher Ca_V channel availability and therefore increased amplitude of the glucose-induced islet Ca^{2+} transients. Supporting the Ca^{2+} toxicity hypothesis is also the observation that L-type Ca^{2+} channel pharmacological inhibition using verapamil delays β cell mass reduction in T1DM and T2DM diabetes patients or mouse models (69–72). In line with these concepts is also the observation that under ER stress conditions islets isolated from female mice showed a greater ability to maintain glucose-stimulated insulin production and secretion caused by higher expression of genes linked with protein synthesis, folding, and processing (60).

Besides controlling the firing frequency, our experiments show that the most important role of $K_V2.1$ currents in male β cells is to maintain a hyperpolarized MP. The question arises as to how a delayed rectifier K^+ channel that should be activated only during an AP can modulate the MP in the absence of the electrical activity. The MP in β cells is characterized by constant oscillations generated by the activation of background depolarizing and hyperpolarizing currents. Depending on the extracellular glucose concentration, the peak of the oscillations might be below the depolarization threshold of the Ca_V and Na_V channels and therefore would not elicit an AP. However, these oscillations could activate a very small percentage of $K_V2.1$ channels. Based on the experimentally determined voltage dependence of activation and inactivation (Figure 5C), we calculate using Boltzmann equations that at –60 mV approximately 2% of $K_V2.1$ current is activated. Considering the sex-specific $K_V2.1$ maximal current densities, this would elicit an approximately 2.62 pA/pF current in males and approximately 1.51 pA/pF current in female β cells. Because Ca^{2+} influx at –60 mV was approximately –1 pA/pF in β cells of both sexes, the larger $K_V2.1$ current would maintain the male β cell MP close to the K^+ reversal potential over a wider range of extracellular glucose concentrations.

This change in MP will also modulate the incretin insulinotropic effects. Recently, it has been shown that persistent β cell membrane depolarization shifts the incretin pathway from G_s to G_q (57). Although female β cells are not continuously depolarized but show only a stronger glucose-dependent MP depolarization, this is sufficient to increase the contribution of the G_q pathway to the GLP-1–induced potentiation while maintaining a similar total incretin response. An additional effect of a partial $K_V2.1$ channel inhibition has previously been demonstrated to be the reduced GLP-1 dose required to trigger an incretin insulinotropic effect, both in isolated healthy islets as well as a diabetes mouse model (42). Therefore, it is very tempting to speculate that due to the more depolarized MP, females might respond with a similar insulinotropic effect compared to males but using a lower dose that will minimize the side effects. Our data also suggest that gastric inhibitory peptide (GIP) will have a reduced effect in females since GIP activates only G_s, while GLP-1 activates both G_s and G_q pathways (57).

Besides their role in membrane hyperpolarization, $K_V2.1$ channels can modulate β cell function and survival through other mechanisms. It has been shown that $K_V2.1$ channels increase vesicle exocytosis via enhanced vesicle recruitment and fusion (44–46). However, our data do not show a sex-specific role of $K_V2.1$ channel in exocytosis since Cm measurements as well as first-phase insulin release were similar in β cells of both sexes. Nevertheless, a structural and sex-specific role of $K_V2.1$ channels has been demonstrated in smooth muscle cells (73). In male myocytes, the $K_V2.1$ channels are expressed at lower levels and mostly involved in membrane hyperpolarization, while in female myocytes $K_V2.1$ channels show higher expression levels but act as an enhancer of $Ca_V1.2$ L-type Ca^{2+} channel clustering and therefore increase Ca^{2+} influx and myogenic tone. Whether $K_V2.1$ channels assume a similar sex-specific structural role in pancreatic β cells remains to be investigated. We also cannot distinguish whether the sex-specific $K_V2.1$ current density is caused by sex hormone–modulated transcriptional regulation, subcellular localization, protein interactions, or posttranslational modifications. Nevertheless, we can exclude an acute effect of sex hormones on $K_V2.1$ gating properties since all our experiments were performed on pancreatic islets and β cells cultured for 24 hours in the absence of any sex hormones.

In addition to the different $K_V2.1$ conductances, the Ca^{2+}-activated BK and SK currents also showed sex-specific properties. In response to a short (90 ms) Ca^{2+}-loading prepulse, the SK component showed a significantly higher amplitude in females compared with males. Functionally, the larger SK currents explain the higher amplitude of the AHP component observed in single APs recorded during the induced electrical activity in response to step current injections. The BK currents had the same amplitude in β cells of both sexes, but showed a significantly faster inactivation in females compared with males following Ca^{2+}-loading prepulses shorter than 810 ms. The faster BK current inactivation could partially be responsible for the increased bursting behavior and burst duration observed in female β cells. However, both SK and BK currents following longer Ca^{2+}-loading prepulses showed the same biophysical properties in β cells of both sexes, suggesting that in pancreatic β cells the sex hormone regulation leads to a different functional coupling between the Ca^{2+} source and the SK or BK K^+ channels.

A caveat of our study is that we performed our analysis on mice 5 to 19 weeks old. Recently it has been shown that sex-specific pancreatic β cell mass and glucose tolerance are age dependent (74). Male mice showed glucose and insulin intolerance comparable to those of females at 3 and 6 months of age, while 6-month-old males displayed increased β cell mass in response to reduced insulin resistance compared with littermate females (74). However, recently a different study reported that until 3 months both male and

female C57BL/6 mice have similar insulin sensitivity (60). Additionally, although the 14-week-old male mice used in our study did show a tendency toward larger islet areas compared with females (male islet size = 0.9 ± 0.11 μm^2, n = 89; female islet size =0.55 ± 0.02 μm^2, n = 566), this difference was not significantly different (Mann-Whitney test P = 0.14). We did not quantify the total β cell mass by multiplying the relative insulin-positive area with pancreas weight. But, important for our study is that the islet area and β cell contribution to islets did not show any significant sex-specific differences and therefore we can assume a similar islet cell paracrine modulation (75–78).

A second limitation of our study is that we performed our analysis only on 1 mouse strain, C57BL/6 × 129J. Several previous studies have demonstrated significant strain-specific differences in mice regarding insulin release (79, 80), pancreas size and structure (81), and susceptibility to diabetes (79–84). However, our findings showing that female islets secrete more insulin that leads to a better glucose tolerance corroborate well both with human data (2, 60–63) and several rodent studies (60, 74, 85). Additionally, a recent study demonstrated (74), also in the C57BL/6 background, that female islets respond with reduced Ca^{2+} transients to glucose stimulation but increased β cell oscillatory responses compared with males, very similar to our previous (48) and current study. Nevertheless, while under basal glucose conditions female islets secreted more insulin, the stimulated insulin release was higher in males (74). The higher insulin release in males could be secondary to already existing altered insulin sensitivity and not directly caused by sex-specific β cell functions. Given the different mouse genetic backgrounds and different experimental conditions between laboratories, it is not surprising that the results are sometimes divergent. However, one constant is that sex plays a critical and very complex role in glucose metabolism, affecting insulin sensitivity, β cell mass and its resilience to diabetes, and insulin synthesis and release.

Our study demonstrates dramatic sex-specific differences in β cell MPs and electrical activity. These differences are primarily caused by significantly different sex-specific $K_V2.1$ current densities. In male mice, the larger $K_V2.1$ currents cause a reduced β cell firing frequency that translates to reduced second-phase insulin release and therefore increased susceptibility to diabetes. In female β cells, the smaller $K_V2.1$ current density causes a stronger glucose-induced membrane depolarization that increases the firing frequency but limits the Ca^{2+} influx due to MP-dependent Ca_V channel inactivation. Under stress conditions, the smaller-amplitude Ca^{2+} transients might limit mitochondrial damage and therefore, increased female β cell resilience. Additional studies are required to investigate how the differences that we observe here might contribute to sex-specific incidence of hyperglycemia in older ages, especially after the onset of insulin resistance.

Methods

Sex as a biological variable. We conducted this study on pancreatic islets and β cells of both male and female mice.

Mouse model. The mouse line has a mixed C57BL/6 × 129J background (48). The mouse colony maintenance and all experiments were performed in conformity with international laws and respected the 3R principle. The data presented in this manuscript did not include any animal experimentation. The number of mice used for tissues collection was regularly reported to the Austrian Ministry of Science (BMWFW).

Islet and β cell isolation. Pancreatic islets from adult mice (5–19 weeks old) were enzymatically isolated as previously reported (48, 86). For electrophysiology, insulin release, and Ca^{2+} imaging recordings the islets were cultured at 37°C and 5% CO_2 overnight in RPMI 1640 medium (11 mM glucose) supplemented with 5% FBS, 2 mM L-glutamine, 100 mg/mL streptomycin, and 100 IU/mL penicillin. For the experiments performed on isolated β cells, the islets were incubated in solution containing (in mM) 138 NaCl, 6 KCl, 3 $MgCl_2$, 5 HEPES, 3 glucose, 1 EGTA, and 1 mg/mL BSA for 12 minutes at 37°C and then mechanically dissociated and cultured as previously described (48, 86).

Solutions for electrophysiology. For membrane potential recordings as well as K_V and K_{ATP} K^+ currents a physiological solution containing (in mM) 140 NaCl, 3.6 KCl, 2 $NaHCO_3$, 0.5 NaH_2PO_4, 0.5 $MgSO_4$, 5 HEPES, 2.5 $CaCl_2$, glucose (2, 5, 7.5, 10, 15, or 20) (pH 7.4 with NaOH) was used. The internal solution consisted of (in mM) 76 K_2SO_4, 10 NaCl, 10 KCl, 1 $MgCl_2$, and 5 HEPES (pH 7.35 with KOH). For K_2P currents, the extracellular solution contained in (in mM) 97.7 *N*-methyl-D-glucamine, 26 KCl, 25 HEPES, 1.2 $MgSO_4$, 1.2 KH_2PO_4, 14.4 glucose, 20 tetraethylammonium chloride (TEA-Cl), and 0.1 tolbutamide (Sigma-Aldrich) (pH 7.35 with NaOH). The intracellular solution was composed of (in mM) 140 KCl, 1 $MgCl_2$, 10 EGTA, and 10 HEPES (pH 7.25 with KOH). For Ca_V currents, the pipette was filled with (in mM) 76 $CsSO_4$, 10 CsCl, 10 KCl, 1 $MgCl_2$, and 5 mM HEPES. For the capacitance measurements, the pipette solution contained (in mM) 140 CsCl, 10 NaCl, 1 $MgCl_2$,

0.05 EGTA, 5 HEPES, 0.1 cAMP, and 0.1 MgATP (pH 7.2 with CsOH). The external solution for Ca_V currents and capacitance measurements contained (in mM) 118 NaCl, 5.6 KCl, 20 TEA-Cl, 1.2 $MgCl_2$, 5 HEPES, 2.6 $CaCl_2$, and 5 glucose (pH 7.4 with NaOH).

Glucose-induced and current injection–induced electrical activity. The electrical activity was measured in current-clamp mode using the HEKA amplifier and the perforated patch-clamp technique (0.24 mg/mL amphotericin B, Sigma-Aldrich) in intact islets maintained at 32°C–34°C by perfusing increasing glucose concentrations (2, 5, 7.5, 10, 15, and 20 mM). β Cells were identified by being active at glucose concentrations above 5 mM and silent at lower concentrations and/or by the steady-state inactivation of Na^+ currents, as previously described (21). To characterize the current-step-induced electrical activity, islets were dispersed to obtain isolated single cells, as previously described (86).

Voltage-clamp experiments. All voltage-clamp experiments were performed at room temperature. The Na_V, BK, SK, K_{ATP} K_2P, and $K_V2.1$ currents were recorded in β cells in intact pancreatic islets. The Ca_V currents were recorded in isolated β cells. The Na_V, Ca_V, BK, SK, and $K_V2.1$ current were subject to online P/4 leak subtraction, while the K_{ATP} and K_2P were not leak subtracted. For this analysis, only recordings with a leak of less than –50 pA were used. The current densities were calculated by dividing the measured current by the Cm that represents a direct measurement of cell area. The Cm did not show a sex-specific difference in all our experiments (Cm_{Males} = 6.74 ± 0.18, n = 78; $Cm_{Females}$ = 7.42 ± 0.23 pF, n = 88; P = 0.09 by Mann-Whitney test). The voltage dependence of the Na^+ current inactivation was used to distinguish the β cells from pancreatic non-β cells (48). K_{ATP} currents were recorded using a double square pulse of ± 10 mV (500 ms long) starting from –70 mV. Diazoxide (340 μM, Sigma-Aldrich) was dissolved in 0.1 mM NaOH solution and was added to the bath solution. For recording 2-pore K^+ channels (K_2P), a 1-second-ramp protocol from –120 mV to +60 mV was applied. The Ca^{2+}-activated K^+ channels and K_v isoforms were pharmacologically dissected using the specific BK (paxilline, 1 μM; Sigma-Aldrich) and SK (apamin, 200 nM; Alomone) blockers. The protocol used for recording Ca^{2+}-activated K^+ channels consists of a Ca^{2+}-loading prepulse to 0 mV that increased its duration by 90 ms every step. The test pulse consisted of a depolarization to +80 mV for 600 ms. To determinate the K_v isoform, we applied the specific $K_v2.1$ blocker Strx-1 (100 nM; Smartox Biotechnology). Ca^{2+} currents were elicited using 200-ms depolarization steps from –80 mV or –50 mV to +60 mV in 10-mV increments and analyzed as previously described (48).

Capacitance measurements. The increase in Cm was recorded in β cells in intact islets bathed at 32°C–33°C using the lock-in and sine+DC mode of the HEKA amplifier. The exocytosis was triggered by a train of 10 depolarizing steps, 500 ms long, from –70 mV to 0 mV.

Ca^{2+} imaging. Intact pancreatic islets were loaded with Fluo-4-AM Ca^{2+} indicator (5 μM; Thermo Fisher Scientific) and 0.1% pluronic acid for 30 minutes at room temperature followed by a 30-minute incubation at 37°C. Single islets were perfused with physiological solution in which Ca^{2+} was 2.5 mM or omitted. Carbachol (0.2 mM; Sigma-Aldrich) was added to deplete the ER by activating IP_3Rs in 0 mM Ca^{2+}–containing extracellular solution.

Dynamic insulin release. For each experiment, 20 islets were perfused with a physiological solution (in mM) of 140 NaCl, 3.6 KCl, 2 $NaHCO_3$, 0.5 NaH_2PO_4, 0.5 $MgSO_4$, 5 HEPES, and 2.5 $CaCl_2$ with different glucose concentrations (2, 5, and 10 mM) at 37°C. The flow rate was set to 200 μL/min and the fractions collected every 2 minutes using an automated system. Insulin concentration in the fractions was measured with an ultrasensitive sandwich ELISA protocol. GLP-1 (1 nM; Bachem) and YM-254890 (100 nM; MedChemExpress) were added where indicated. To allow a direct comparison between different experiments, the insulin release per islet and unit of time was calculated based on islet area (87) and flow rate respectively. A picture of all the islets was obtained before the experiment using the Moticam 2500 camera connected to a fixed-focus dissection microscope. The area was calculated using the proprietary Moticam software that incorporates a calibrated distance measurement. The insulin concentration was multiplied by the correction factor representing the relative difference in islet area compared with the area of the largest islet group measured in all experiments.

Statistics. Data analysis was performed using FitMaster (Heka), Clampfit 10.7 (Axon Instruments), SigmaPlot 13 (Systat Software, Inc.), Origin (2021b), or GraphPad Prism (8.01). All values are presented as mean ± SEM for the indicated number of cells (n), except where stated otherwise. For all experiments, a minimum of 3 mice per sex were used. Statistical significance was calculated using paired or unpaired Student's t test, Mann-Whitney test, or 1-way ANOVA followed by Bonferroni's post hoc test.

Data and materials availability. All analyzed data are available in the main text. The raw data can be found in the Supporting Data Values file in the supplemental material.

Author contributions

NJP and PT conceptualized the study. NJP, TT, SMG, and PT developed the methodology. NJP and TT carried out experiments. NJP and PT generated figures. PT supervised the study. NJP wrote the original draft of the manuscript, which was reviewed and edited by NJP and PT.

Acknowledgments

This research was funded in whole by the Austrian Science Fund (FWF) (grants 10.55776/P31434, 10.55776/P36053, and 10.55776/DOC30).

Address correspondence to: Petronel Tuluc, Pharmacology and Toxicology, Institute of Pharmacy, University of Innsbruck, Innrain 80-82/III, A-6020 Innsbruck, Austria. Phone: 4351250758805; E-mail: petronel.tuluc@uibk.ac.at.

1. Kautzky-Willer A, et al. Sex and gender differences in risk, pathophysiology and complications of type 2 diabetes mellitus. *Endocr Rev*. 2016;37(3):278–316.
2. Nordstrom A, et al. Higher prevalence of type 2 diabetes in men than in women is associated with differences in visceral fat mass. *J Clin Endocrinol Metab*. 2016;101(10):3740–3746.
3. Mauvais-Jarvis F, et al. The role of estrogens in pancreatic islet physiopathology. *Adv Exp Med Biol*. 2017;1043:385–399.
4. Mauvais-Jarvis F. Gender differences in glucose homeostasis and diabetes. *Physiol Behav*. 2018;187:20–23.
5. Liu S, et al. Importance of extranuclear estrogen receptor-alpha and membrane G protein-coupled estrogen receptor in pancreatic islet survival. *Diabetes*. 2009;58(10):2292–2302.
6. Rees DA, Alcolado JC. Animal models of diabetes mellitus. *Diabet Med*. 2005;22(4):359–370.
7. Franconi F, et al. Are the available experimental models of type 2 diabetes appropriate for a gender perspective? *Pharmacol Res*. 2008;57(1):6–18.
8. Gannon M, et al. Sex differences underlying pancreatic islet biology and its dysfunction. *Mol Metab*. 2018;15:82–91.
9. Flanagan DE, et al. Gender differences in the relationship between leptin, insulin resistance and the autonomic nervous system. *Regul Pept*. 2007;140(1-2):37–42.
10. Rorsman P, et al. Regulation of calcium in pancreatic α- and β-cells in health and disease. *Cell Calcium*. 2012;51(3–4):300–308.
11. Gandasi NR, et al. Ca^{2+} channel clustering with insulin-containing granules is disturbed in type 2 diabetes. *J Clin Invest*. 2017;127(6):2353–2364.
12. Rorsman P, Ashcroft FM. Pancreatic β-cell electrical activity and insulin secretion: of mice and men. *Physiol Rev*. 2018;98(1):117–214.
13. Yang SN, Berggren PO. The role of voltage-gated calcium channels in pancreatic beta-cell physiology and pathophysiology. *Endocr Rev*. 2006;27(6):621–676.
14. Tuluc P, et al. Role of high voltage-gated Ca^{2+} channel subunits in pancreatic β-cell insulin release. From structure to function. *Cells*. 2021;10(8):2004.
15. Ashcroft FM, et al. Glucose induces closure of single potassium channels in isolated rat pancreatic beta-cells. *Nature*. 1984;312(5993):446–448.
16. Ashcroft FM, Rorsman P. K(ATP) channels and islet hormone secretion: new insights and controversies. *Nat Rev Endocrinol*. 2013;9(11):660–669.
17. Sakura H, et al. Glucose modulation of ATP-sensitive K-currents in wild-type, homozygous and heterozygous glucokinase knock-out mice. *Diabetologia*. 1998;41(6):654–659.
18. Dadi PK, et al. Pancreatic β-cell-specific ablation of TASK-1 channels augments glucose-stimulated calcium entry and insulin secretion, improving glucose tolerance. *Endocrinology*. 2014;155(10):3757–3768.
19. Vierra NC, et al. Type 2 diabetes-associated K^+ channel TALK-1 modulates β-cell electrical excitability, second-phase insulin secretion, and glucose homeostasis. *Diabetes*. 2015;64(11):3818–3828.
20. Arkhammar P, et al. Inhibition of ATP-regulated K^+ channels precedes depolarization-induced increase in cytoplasmic free Ca^{2+} concentration in pancreatic beta-cells. *J Biol Chem*. 1987;262(12):5448–5454.
21. Gopel S, et al. Voltage-gated and resting membrane currents recorded from B-cells in intact mouse pancreatic islets. *J Physiol*. 1999;521 Pt 3(pt 3):717–728.
22. Porte D Jr., Pupo AA. Insulin responses to glucose: evidence for a two pool system in man. *J Clin Invest*. 1969;48(12):2309–2319.
23. Kanno T, et al. Large dense-core vesicle exocytosis in pancreatic beta-cells monitored by capacitance measurements. *Methods*. 2004;33(4):302–311.
24. Olofsson CS, et al. Fast insulin secretion reflects exocytosis of docked granules in mouse pancreatic B-cells. *Pflugers Arch*. 2002;444(1–2):43–51.
25. Barg S, et al. A subset of 50 secretory granules in close contact with L-type Ca^{2+} channels accounts for first-phase insulin secretion in mouse beta-cells. *Diabetes*. 2002;51 Suppl 1:S74–S82.
26. Barg S, et al. Fast exocytosis with few Ca(2+) channels in insulin-secreting mouse pancreatic B cells. *Biophys J*. 2001;81(6):3308–3323.
27. Bokvist K, et al. Co-localization of L-type Ca^{2+} channels and insulin-containing secretory granules and its significance for the

initiation of exocytosis in mouse pancreatic B-cells. *EMBO J*. 1995;14(1):50–57.
28. Schulla V, et al. Impaired insulin secretion and glucose tolerance in beta cell-selective Ca(v)1.2 Ca^{2+} channel null mice. *EMBO J*. 2003;22(15):3844–3854.
29. Rorsman P, et al. Electrophysiology of pancreatic β-cells in intact mouse islets of Langerhans. *Prog Biophys Mol Biol*. 2011;107(2):224–235.
30. Atwater I, et al. Mouse pancreatic beta-cells: tetraethylammonium blockage of the potassium permeability increase induced by depolarization. *J Physiol*. 1979;288:561–574.
31. Henquin JC, Meissner HP. Significance of ionic fluxes and changes in membrane potential for stimulus-secretion coupling in pancreatic B-cells. *Experientia*. 1984;40(10):1043–1052.
32. Jacobson DA, et al. Kv2.1 ablation alters glucose-induced islet electrical activity, enhancing insulin secretion. *Cell Metab*. 2007;6(3):229–235.
33. Goforth PB, et al. Calcium-activated K^+ channels of mouse beta-cells are controlled by both store and cytoplasmic Ca^{2+}: experimental and theoretical studies. *J Gen Physiol*. 2002;120(3):307–322.
34. Houamed KM, et al. BK channels mediate a novel ionic mechanism that regulates glucose-dependent electrical activity and insulin secretion in mouse pancreatic β-cells. *J Physiol*. 2010;588(pt 18):3511–3523.
35. Jacobson DA, et al. Calcium-activated and voltage-gated potassium channels of the pancreatic islet impart distinct and complementary roles during secretagogue induced electrical responses. *J Physiol*. 2010;588(pt 18):3525–3537.
36. Thompson B, Satin LS. Beta-cell ion channels and their role in regulating insulin secretion. *Compr Physiol*. 2021;11(4):1–21.
37. MacDonald PE, et al. Inhibition of Kv2.1 voltage-dependent K^+ channels in pancreatic beta-cells enhances glucose-dependent insulin secretion. *J Biol Chem*. 2002;277(47):44938–44945.
38. Yan L, et al. Expression of voltage-gated potassium channels in human and rhesus pancreatic islets. *Diabetes*. 2004;53(3):597–607.
39. Smith PA, et al. Delayed rectifying and calcium-activated K^+ channels and their significance for action potential repolarization in mouse pancreatic beta-cells. *J Gen Physiol*. 1990;95(6):1041–1059.
40. Herrington J. Gating modifier peptides as probes of pancreatic beta-cell physiology. *Toxicon*. 2007;49(2):231–238.
41. Li XN, et al. The role of voltage-gated potassium channels Kv2.1 and Kv2.2 in the regulation of insulin and somatostatin release from pancreatic islets. *J Pharmacol Exp Ther*. 2013;344(2):407–416.
42. Sukma Rita R, et al. Partial blockade of Kv2.1 channel potentiates GLP-1's insulinotropic effects in islets and reduces its dose required for improving glucose tolerance in type 2 diabetic male mice. *Endocrinology*. 2015;156(1):114–123.
43. Zhou TT, et al. SP6616 as a new Kv2.1 channel inhibitor efficiently promotes β-cell survival involving both PKC/Erk1/2 and CaM/PI3K/Akt signaling pathways. *Cell Death Dis*. 2016;7(5):e2216.
44. Dai XQ, et al. The voltage-dependent potassium channel subunit Kv2.1 regulates insulin secretion from rodent and human islets independently of its electrical function. *Diabetologia*. 2012;55(6):1709–1720.
45. Fu J, et al. Kv2.1 Clustering contributes to insulin exocytosis and rescues human β-cell dysfunction. *Diabetes*. 2017;66(7):1890–1900.
46. Greitzer-Antes D, et al. K_v2.1 clusters on β-cell plasma membrane act as reservoirs that replenish pools of newcomer insulin granule through their interaction with syntaxin-3. *J Biol Chem*. 2018;293(18):6893–6904.
47. Kim SJ, et al. Pancreatic β-cell prosurvival effects of the incretin hormones involve post-translational modification of Kv2.1 delayed rectifier channels. *Cell Death Differ*. 2012;19(2):333–344.
48. Mastrolia V, et al. Loss of $\alpha_2\delta$-1 calcium channel subunit function increases the susceptibility for diabetes. *Diabetes*. 2017;66(4):897–907.
49. Braun M, et al. Voltage-gated ion channels in human pancreatic beta-cells: electrophysiological characterization and role in insulin secretion. *Diabetes*. 2008;57(6):1618–1628.
50. Riz M, et al. Mathematical modeling of heterogeneous electrophysiological responses in human β-cells. *PLoS Comput Biol*. 2014;10(1):e1003389.
51. Andres MA, et al. Depletion of SK1 channel subunits leads to constitutive insulin secretion. *FEBS Lett*. 2009;583(2):369–376.
52. Gopel SO, et al. Activation of Ca(2+)-dependent K(+) channels contributes to rhythmic firing of action potentials in mouse pancreatic beta cells. *J Gen Physiol*. 1999;114(6):759–770.
53. Tamarina NA, et al. Small-conductance calcium-activated K^+ channels are expressed in pancreatic islets and regulate glucose responses. *Diabetes*. 2003;52(8):2000–2006.
54. Zhang M, et al. Pharmacological properties and functional role of Kslow current in mouse pancreatic beta-cells: SK channels contribute to Kslow tail current and modulate insulin secretion. *J Gen Physiol*. 2005;126(4):353–363.
55. Cheng YM, et al. Molecular determinants of U-type inactivation in Kv2.1 channels. *Biophys J*. 2011;101(3):651–661.
56. MacDonald PE, et al. Members of the Kv1 and Kv2 voltage-dependent K(+) channel families regulate insulin secretion. *Mol Endocrinol*. 2001;15(8):1423–1435.
57. Oduori OS, et al. Gs/Gq signaling switch in β cells defines incretin effectiveness in diabetes. *J Clin Invest*. 2020;130(12):6639–6655.
58. Zhang IX, et al. ER stress increases store-operated Ca^{2+} entry (SOCE) and augments basal insulin secretion in pancreatic beta cells. *J Biol Chem*. 2020;295(17):5685–5700.
59. Kono T, et al. Impaired store-operated calcium entry and STIM1 loss lead to reduced insulin secretion and increased endoplasmic reticulum stress in the diabetic β-cell. *Diabetes*. 2018;67(11):2293–2304.
60. Brownrigg GP, et al. Sex differences in islet stress responses support female β cell resilience. *Mol Metab*. 2023;69:101678.
61. Tura A, et al. Sex- and age-related differences of metabolic parameters in impaired glucose metabolism and type 2 diabetes compared to normal glucose tolerance. *Diabetes Res Clin Pract*. 2018;146:67–75.
62. Horie I, et al. Sex differences in insulin and glucagon responses for glucose homeostasis in young healthy Japanese adults. *J Diabetes Investig*. 2018;9(6):1283–1287.
63. Hall E, et al. Sex differences in the genome-wide DNA methylation pattern and impact on gene expression, microRNA levels and insulin secretion in human pancreatic islets. *Genome Biol*. 2014;15(12):522.
64. Kautzky-Willer A, et al. Influence of increasing BMI on insulin sensitivity and secretion in normotolerant men and women of a wide age span. *Obesity (Silver Spring)*. 2012;20(10):1966–1973.
65. Basu R, et al. Effects of age and sex on postprandial glucose metabolism: differences in glucose turnover, insulin secretion, insulin

action, and hepatic insulin extraction. *Diabetes*. 2006;55(7):2001–2014.
66. Yang SN, et al. Ionic mechanisms in pancreatic β cell signaling. *Cell Mol Life Sci*. 2014;71(21):4149–4177.
67. Santos GJ, et al. Metabolic memory of β-cells controls insulin secretion and is mediated by CaMKII. *Mol Metab*. 2014;3(4):484–489.
68. Dadi PK, et al. Inhibition of pancreatic β-cell Ca^{2+}/calmodulin-dependent protein kinase II reduces glucose-stimulated calcium influx and insulin secretion, impairing glucose tolerance. *J Biol Chem*. 2014;289(18):12435–12445.
69. Ovalle F, et al. Verapamil and beta cell function in adults with recent-onset type 1 diabetes. *Nat Med*. 2018;24(8):1108–1112.
70. Khodneva Y, et al. Calcium channel blocker use is associated with lower fasting serum glucose among adults with diabetes from the REGARDS study. *Diabetes Res Clin Pract*. 2016;115:115–121.
71. Xu G, et al. Preventing β-cell loss and diabetes with calcium channel blockers. *Diabetes*. 2012;61(4):848–856.
72. Forlenza GP, et al. Effect of verapamil on pancreatic beta cell function in newly diagnosed pediatric type 1 diabetes: a randomized clinical trial. *JAMA*. 2023;329(12):990–999.
73. O'Dwyer SC, et al. Kv2.1 channels play opposing roles in regulating membrane potential, Ca^{2+} channel function, and myogenic tone in arterial smooth muscle. *Proc Natl Acad Sci U S A*. 2020;117(7):3858–3866.
74. Jo S, et al. Sex differences in pancreatic β-cell physiology and glucose homeostasis in C57BL/6J mice. *J Endocr Soc*. 2023;7(9):bvad099.
75. Huang JL, et al. Paracrine signalling by pancreatic δ cells determines the glycaemic set point in mice. *Nat Metab*. 2024;6(1):61–77.
76. Vergari E, et al. Somatostatin secretion by Na^{+}-dependent Ca^{2+}-induced Ca^{2+} release in pancreatic delta-cells. *Nat Metab*. 2020;2(1):32–40.
77. Satin LS, et al. "Take me to your leader": an electrophysiological appraisal of the role of hub cells in pancreatic islets. *Diabetes*. 2020;69(5):830–836.
78. Rorsman P, Huising MO. The somatostatin-secreting pancreatic δ-cell in health and disease. *Nat Rev Endocrinol*. 2018;14(7):404–414.
79. Mitok KA, et al. Islet proteomics reveals genetic variation in dopamine production resulting in altered insulin secretion. *J Biol Chem*. 2018;293(16):5860–5877.
80. Berglund ED, et al. Glucose metabolism in vivo in four commonly used inbred mouse strains. *Diabetes*. 2008;57(7):1790–1799.
81. Bock T, et al. Genetic background determines the size and structure of the endocrine pancreas. *Diabetes*. 2005;54(1):133–137.
82. Cruciani-Guglielmacci C, et al. Molecular phenotyping of multiple mouse strains under metabolic challenge uncovers a role for Elovl2 in glucose-induced insulin secretion. *Mol Metab*. 2017;6(4):340–351.
83. Svensson C, et al. Lack of long-term beta-cell glucotoxicity in vitro in pancreatic islets isolated from two mouse strains (C57BL/6J; C57BL/KsJ) with different sensitivities of the beta-cells to hyperglycaemia in vivo. *J Endocrinol*. 1993;136(2):289–296.
84. West DB, et al. Dietary obesity in nine inbred mouse strains. *Am J Physiol*. 1992;262(6 pt 2):R1025–R1032.
85. Li T, et al. Sex effect on insulin secretion and mitochondrial function in pancreatic beta cells of elderly Wistar rats. *Endocr Res*. 2016;41(3):167–179.
86. Jing X, et al. CaV2.3 calcium channels control second-phase insulin release. *J Clin Invest*. 2005;115(1):146–154.
87. Slepchenko KG, et al. Comparing methods to normalize insulin secretion shows the process may not be needed [published online March 1, 2019]. *J Endocrinol*. https://doi.org/10.1530/JOE-18-0542.